

Ultimate Power of Inference Attacks: Privacy Risks of High-Dimensional Models

Sasi Kumar Murakonda
murakond@comp.nus.edu.sg
National University of Singapore

Reza Shokri
reza@comp.nus.edu.sg
National University of Singapore

George Theodorakopoulos
TheodorakopoulosG@cardiff.ac.uk
Cardiff University

ABSTRACT

Models leak information about their training data. This enables attackers to infer sensitive information about their training sets, notably determine if a data sample was part of the model’s training set. The existing works *empirically* show the *possibility* of these tracing (membership inference) attacks against complex models with a large number of parameters. However, the attack results are dependent on the specific training data, can be obtained only after the tedious process of training the model and performing the attack, and are missing any measure of the confidence and unused potential power of the attack. A model designer is interested in identifying which model structures leak more information, how adding new parameters to the model increases its privacy risk, and what is the gain of adding new data points to decrease the overall information leakage. The privacy analysis should also enable designing the most powerful inference attack.

In this paper, we design a *theoretical* framework to analyze the maximum power of tracing attacks against high-dimensional models, with the focus on probabilistic graphical models. We provide a tight upper-bound on the power (true positive rate) of these attacks, with respect to their error (false positive rate). The bound, as it should be, is independent of the knowledge and algorithm of any specific attack, as well as the values of particular samples in the training set. It provides a measure of the potential leakage of a model given its structure, as a function of the structure complexity and the size of training set.

1 INTRODUCTION

How much is the privacy risk of releasing high-dimensional models which are trained on sensitive data? We focus on measuring information leakage of models about their training data, using tracing (membership inference) attacks. Given the released model and a target data sample, the adversary aims at inferring whether or not the target sample was a member of the training set. We use the term tracing attack and membership inference attack interchangeably. The attack is evaluated based on its power (true positive rate), and its error (false positive rate), in its binary decisional task.

Tracing attacks have been extensively studied for summary statistics, where independent statistics (e.g., mean) of attributes of high-dimensional data are released. Although initial works showed the existence of powerful tracing attacks [10], more recent work provided theoretical frameworks to analyze the upper bound on the power of these inference attacks [20], and their robustness to noisy statistics [7]. The theoretical analysis helps reason about the major causes of information leakage and their influence on the power of the membership inference attacks. However, the analysis is limited to simple models such as product distributions.

Advanced machine learning algorithms, such as deep neural networks, have recently been tested against tracing attacks. In the black-box setting, the attacker can only observe predictions of the model. The attack involves training inference models that can distinguish between members and non-members from the predictions that the target model produces [21]. The attacks are tested against deep neural networks as well as machine-learning-as-a-service platforms, and their accuracy is shown to be related to their generalization error [21, 23]. In the white-box setting, the attacker obtains the parameters of the model, and decides that the target sample is a member if the gradients of the loss with respect to the model’s parameters computed on the target data sample are aligned with the model’s parameters [17]. Large models are empirically shown to be more vulnerable to the attack, even if they have a better generalization performance. These attacks highlight the susceptibility of high-dimensional neural networks to tracing attacks. However, their analysis is limited to empirical measurements of the attack success on particular data sets.

Contributions. Using the above-mentioned existing methods, it is possible to reason theoretically about tracing attacks, yet only for extremely simple models (independent statistics). In parallel, it is possible to perform empirical tracing attacks against complex models (deep neural networks), yet without much theoretical analysis. In this paper, we aim at closing this gap by providing a theoretical framework for reasoning about tracing attacks against high dimensional models, i.e. models with many parameters. With this framework, one can compute the power and error of an attack, compute the tradeoff between power and error for various attack choices, design the most powerful attack for a given error, and also determine the elements of a released model that contribute to the power/error of the attacker. Our focus is on *probabilistic graphical models*, which are very general statistical models that capture the correlations among attributes of data, and are among fundamental models for machine learning, and the basis of many deep learning models via e.g. restricted Boltzmann machines.

We use the likelihood ratio test (LR test) as the foundation of our tracing attack [20]. This enables us to **design the most powerful attack** against any probabilistic model. Thus, for any given error, there exist no other attack strategy that can achieve a higher power. Our objective is not to empirically evaluate the performance of attacks (even the theoretically strongest one) on trained models. We **compute the maximum achievable power of tracing attacks**. This upper bound can be used as a measure to evaluate the effectiveness of different attack algorithms by comparing their achieved power to the bound for any false positive error.

Our objective is to identify the elements of a model that cause membership information leakage, and measure their influence. We prove that, for a given model structure, the potential leakage of the

model (the leakage that corresponds to the most powerful attack for any given error) is proportional to the square root of model’s complexity (as the number of its independent parameters), and is inversely proportional to the square root of size of training set. Thus, the theoretical bound enables us to **quantify the potential leakage of a model before even learning the parameters of the model** on that structure. This can be used to efficiently compare different model structures based on their susceptibility to tracing attacks. This is of significant value when choosing among various model structures that have comparable utilities. The theoretical bound can quantify the power that the attack gains/loses if a new attribute is added/removed from the data, or when the model requires capturing/removing the correlation between certain set of attributes. It also determines the size of the training set for a very high-dimensional model that leaks a similar amount of information as a small model leaks on a small set of data.

We evaluate our framework against real (sensitive) data: location check-ins, purchase history, and genome data. We empirically show that the upper bound is tight, and power of the likelihood ratio test attacker is extremely close to the bound, for any false positive error. In the experiments, we show that the bound is the same for two model structures of similar dimension, regardless of how the structures are constructed (e.g., using an optimal structure learning algorithm, or totally at random). We also show that independent data samples from the general population are enough to build a strong attack, and the attacker is not required to learn about the true generative model for his dataset.

2 PROBABILISTIC GRAPHICAL MODELS

In a multi-dimensional space, where the probability distribution over each dimension can be represented by a random variable, probabilistic graphical models capture the probability distribution over the space [15]. Probabilistic graphical models have many applications in machine learning, in a variety of domains. They are also the foundation of many advanced machine models, such as the restricted Boltzman machines (used in deep learning).

Probabilistic graphical models make use of a graph-based representation to encode the dependencies and conditional independence between the random variables. Each node X_i in a graph G is a random variable, and the edges represent the dependencies. Bayesian networks and Markov random fields are the most common types of probabilistic graphical models. In this paper, we focus on **Bayesian networks**. However, our attack framework is easily applicable to Markov random fields.

In the Bayesian networks, the model structure is a directed acyclic graph, and the model $\langle G, \theta \rangle$ enables factoring the joint probability over the random variables. Given all its parents in the graph, a random variable becomes conditionally independent of other random variables. Therefore, the joint distribution can be factored as follows.

$$\Pr[X_1, X_2, \dots, X_m] = \prod_{i=1}^m \Pr[X_i | Pa_{X_i}^G; \theta], \quad (1)$$

where $Pa_{X_i}^G; \theta$ is the parent random variables of X_i . The parameters of the model encode the conditional probabilities.

We define the **complexity** C of a Bayesian network $\langle G, \theta \rangle$ with discrete random variables as the number of independent parameters used to define its probability distribution. Let $V(X)$ be the number of distinct values that a random variable X can take. For each conditional probability $\Pr[X_i | Pa_{X_i}^G; \theta]$, we need $|V(Pa_{X_i}^G)|(|V(X_i)| - 1)$ independent parameters. Thus, the total complexity of a model is:

$$C(\langle G, \theta \rangle) = \sum_{i=1}^m |V(Pa_{X_i}^G)|(|V(X_i)| - 1). \quad (2)$$

As a special case, when all the attributes are binary, the model complexity is equal to $\sum_{i=1}^m 2^{|Pa_{X_i}^G|}$.

Given a multi-dimensional dataset, the training algorithm for graphical models involve learning the structure of the model as well as its parameters. Ideally, both the structure learning and parameter learning need to be done using a joint optimization that maximizes the likelihood of data points in the training set. However, due to its high computational complexity, they are optimized in sequence. In this section, our goal is not to provide a comprehensive overview (see [15] if interested), but rather a brief description of the methods for learning structure and parameters of a Bayesian network in a systematic way.

2.1 Structure Learning

The objective is to learn the significant dependencies between random variables, and represent them as a graph. We present an existing algorithm based on maximizing a score function that measures how correlated different attributes are, according to the training data [9]. For each attribute we find a set of attributes which are highly correlated with it, yet are not significantly correlated among themselves.

$$score(Pa_{X_i}^G) = \frac{\sum_{X_j \in Pa_{X_i}^G} corr(X_i, X_j)}{\sqrt{|Pa_{X_i}^G| + \sum_{X_j, X_k \in Pa_{X_i}^G} corr(X_j, X_k)}} \quad (3)$$

While optimizing this score for each attribute, we need to make sure that the graph remains acyclic. Also, to control the complexity of the graph, we impose a condition on η , the maximum number of parents for each node. The structure learning is an iterative and greedy algorithm that adds parents to each node while maximizing the score for all nodes at each iteration, subject to the constraints.

Note that the structure learning might involve expert knowledge, and is not always totally dependent on the training data. It could also be the result of the consensus of a community (e.g., genomicists) on the correlation and dependency between attributes of a particular type of data.

2.2 Parameter Learning

We assume a prior distribution on all possible values of the parameters θ , and use the training data set to update this distribution, using a Bayesian approach.

Let X_i be the random variable for a categorical attribute. Let $\vec{\theta}_i$ be the parameters of the conditional probability $\Pr[X_i | Pa_{X_i}^G; \theta]$. For each assignment of values to $Pa_{X_i}^G; \theta$, we assume a prior distribution on all the possible k -dimensional multinomial distributions. The

Symbol	Description
m	Number of attributes
n	Pool (training set) size
$\langle G, \hat{\theta} \rangle$	Released Model
$\langle G, \theta \rangle$	Population Model
X_i	Random variable for attribute i
x_i	Particular value for X_i
$V(X_i)$	Set of possible values of attribute i
$Pa_{X_i}^G$	Set of random variables that are parents of node X_i in G
p_i^v	$\Pr(x_i = 1 Pa_{X_i}^G = v; \theta)$
\hat{p}_i^v	$\Pr(x_i = 1 Pa_{X_i}^G = v; \hat{\theta})$
$C(G)$	Complexity of G (number of independent parameters)
η	Maximum number of parents per node in G
$L(x)$	Log-likelihood ratio statistic (5) for data sample x
F	CDF of $L(x)$ over the general population (under H_{OUT})
α	Error (False Positive Rate) of LR tracing attack
β	Power (True Positive Rate) of LR tracing attack
z_s	Quantile at level $1 - s$ of the Standard Normal distribution

Table 1: Notations

prior distribution for each assignment v comes from a Dirichlet family, i.e., $\hat{\theta}_i^v \sim \text{Dirichlet}(\vec{\alpha}_i^v)$, where $\vec{\alpha}_i^v$ is the hyper parameters of the distribution (usually set to 1 for all dimensions, which models a uniform prior).

Let $\vec{c}_i^v = [c_{i1}^v, c_{i2}^v, \dots, c_{ik}^v]$ include the frequency of the events $[X_i = j | Pa_{X_i}^G; \theta = v]$ in training data. We compute the posterior distribution for $\hat{\theta}_i^v$ as $\text{Dirichlet}(\vec{\alpha}_i^v + \vec{c}_i^v)$. Thus, the most likely estimation for set of parameters $\hat{\theta}_i^v$ is:

$$\theta_{ij}^v = \frac{\alpha_{ij}^v + c_{ij}^v}{\sum_{j=1}^k (\alpha_{ij}^v + c_{ij}^v)}. \quad (4)$$

As the parameters of the Bayesian network are learned from the training data, they might leak information about the members of the training set.

2.3 Data Synthesis

The graphical models could be used for inference and prediction, as well as generating synthetic data (from the underlying distribution that they encode). Given a data set D , we want to synthesize datasets that are close in distribution to D . The process of generating one synthetic dataset involves the following steps:

- (1) Learn a Bayesian network $\langle G, \theta \rangle$ from the data set D .
- (2) Create a Bayesian network $\langle G', \theta' \rangle$ with $G' = G$, and θ' drawn from the posterior Dirichlet distribution for θ , which was computed during parameter learning.
- (3) Draw independent samples from $\langle G', \theta' \rangle$.

3 PROBLEM STATEMENT

We consider a set of n independent m -dimensional data samples from a *population*. We refer to this set as the *pool*. We do not make any assumption about the probability distribution of the data points in the general population. Given a graphical model structure G , the pool data is used to train a graphical model, i.e., to estimate the parameters $\hat{\theta}$ of the probabilistic graphical **model** $\langle G, \hat{\theta} \rangle$. This

model is *released*. Our objective is to quantify the privacy risks of releasing such models for the members of their training data.

Let us consider an adversary who observes the released model $\langle G, \hat{\theta} \rangle$. We assume that the attacker can collect a set of independent samples from the population. We refer to this set as the *reference population*. The objective of the adversary is to perform a **tracing attack** (also known as the membership inference attack) against the released model, on any target data point x : create a decision rule that determines whether x was used in the training of the parameters of $\langle G, \hat{\theta} \rangle$ or not, i.e. to classify x as being in the pool (IN) or not (OUT).

The accuracy of tracing attack indicates the information leakage of the model about the members of its training set. We quantify the attacker’s success using two evaluation metrics: the adversary’s **power** (the true positive rate), and his **error** (the false positive rate). The power measures the conditional probability that the attacker classifies x as IN, given that x is indeed in the pool, i.e. $\Pr[IN|x \in \text{pool}]$. The error measures the conditional probability that the attacker classifies x as IN, given that x is not in the pool, i.e. $\Pr[IN|x \notin \text{pool}]$. It is not generally possible to maximize both of these metrics at once, and usually there is a trade-off between power and error. The ROC curve (Receiver Operating Characteristic), which is a plot of power versus error, captures this trade-off for an attack. Thus, the area under the ROC curve (AUC) is a single metric for combining the two metrics and measuring the strength of the attack. The AUC can be interpreted as the probability that a randomly drawn data point from the pool will be assigned larger probability of being IN than a data point randomly drawn from outside the pool. So $\text{AUC} = 1$ implies that the attacker can correctly classify all data samples as IN or OUT.

4 FRAMEWORK FOR ATTACK DESIGN

We model the decisional problem of the tracing attack as a hypothesis test, as in the prior work [10, 20]. Given the released model, the reference population, and the target data point, the adversary aims at distinguishing between two hypothesis. Each hypothesis describes a possible world that could have resulted in the observation of the adversary, where in one world the target data was part of the pool, and in the other was not.

- Null hypothesis (H_{OUT}): The pool is constructed by drawing n independent samples from the general population. The parameters $\hat{\theta}$ of the model $\langle G, \hat{\theta} \rangle$ are trained on the pool data. The target data x is drawn from the general population, independently from the pool.
- Alternative hypothesis (H_{IN}): The pool is constructed by drawing n independent samples from the general population. The parameters $\hat{\theta}$ of the model $\langle G, \hat{\theta} \rangle$ are trained on the pool data. The target data x is drawn from pool.

This generalizes the hypothesis test designed by Sankararaman et al. [20], in which the released model follows a product distribution, i.e. the random variables corresponding to data attributes are independent (equivalent to a probabilistic graphical model without any dependency edges between the nodes).

The adversary compares the likelihood of the released model, pool data and the target individual under each hypothesis, and uses the **likelihood ratio test** to decide on the membership of the

target data. The likelihood of the pool data is the same in both hypothesis. Thus, the test is reduced to comparing the likelihood of the target data x under H_{OUT} versus H_{IN} , given the released model.

The adversary should collect the most relevant information from the population data that can help him distinguish between the two hypothesis. This depends on the exact computations that led to the released model. The parameters of the released model are the only information that the adversary has about the pool data, and can leverage to distinguish samples in pool from random samples from the population. Thus, the adversary needs to replicate the exact same computation on the entire reference population. Let θ be the result of this computation, i.e., the parameters of model G trained on the large reference population. The differences between θ and $\hat{\theta}$ is due to the influence of individual members of the pool in the training process. This is what the attacker exploits. So, the model $\langle G, \theta \rangle$ learned from reference population will be used for computing the likelihood of x under H_{OUT} .

To further elaborate the importance of $\langle G, \theta \rangle$, note that if the attacker chooses a model structure that is less complex than the released model structure, then he won't be able to exploit all the released information (in $\langle G, \hat{\theta} \rangle$) about the pool. Similarly, if he chooses a model structure that is more complex than the released model, he won't be able to utilize the additional parameters, as the corresponding statistics for the pool are not available. Hence the optimal choice for the adversary is to compute the parameters of *the released model structure* on the population data.

Finally, the log likelihood statistic is computed as follows.

$$L(x) = \log \left(\frac{\Pr[x; H_{\text{OUT}}]}{\Pr[x; H_{\text{IN}}]} \right) = \log \left(\frac{\Pr[x; \langle G, \theta \rangle]}{\Pr[x; \langle G, \hat{\theta} \rangle]} \right) \quad (5)$$

The LR test is a comparison of the log likelihood statistic $L(x)$ with a threshold. If $L(x) \leq \text{threshold}$, then the attacker decides in favor of H_{IN} (rejects H_{OUT}); otherwise, in favor of H_{OUT} (more precisely, in this case, he fails to reject H_{OUT} because there is not enough evidence to support this rejection in favor of H_{IN}).

To determine the threshold, the attacker selects a (false positive rate) error α that he is willing to tolerate. He then empirically or theoretically estimates the distribution of $L(x)$ under the null hypothesis, using his reference population. We denote the CDF of this distribution as F . Given α and F , the attacker computes a threshold value $F^{-1}(\alpha)$ and compares it to $L(x)$, to decide about rejecting the null hypothesis. This concludes the hypothesis test.

The *power* of the test, as defined earlier, can be expressed as $\Pr[L(x) \leq F^{-1}(\alpha)]$, computed under the alternative hypothesis, for an individual data point x randomly drawn from the pool. In other words, it is the fraction of pool data points that are correctly classified by the test. By varying α , and thus the threshold $F^{-1}(\alpha)$, we can draw the ROC curve and compute the AUC metric as well. It is worth emphasizing that according to the Neyman-Pearson lemma [18], the LR test achieves the **maximum power** among all decision rules with a given error (false positive rate). So, any other decision rule would result in a lower AUC.

5 THEORETICAL FRAMEWORK FOR ATTACK ANALYSIS

Our objective is to compute the maximum power β for any false positive error α of an adversary that observes the released model $\langle G, \hat{\theta} \rangle$ which has been trained on a pool of size n . In our main result, Theorem 1, we show which combinations of α and β are possible for the attacker, and we find the major factors that matter for determining these combinations, as a function of the model complexity and size of the dataset.

THEOREM 1. *Let β and α be the power and error of the LR test, for the membership inference attack, respectively. Let n be the size of the pool (model's training set), and $C(G)$ be the complexity of the released probabilistic graphical model $\langle G, \hat{\theta} \rangle$. Then, the tradeoff between power and error follows the following relation:*

$$z_\alpha + z_{1-\beta} \approx \sqrt{\frac{C(G)}{n}}, \quad (6)$$

where z_s is the quantile at level $1 - s$, $0 < s < 1$ of the Standard Normal distribution.

PROOF SKETCH. To compute $\beta = \Pr_{\text{pool}}\{L(x) \leq F^{-1}(\alpha)\}$, the power of the LR test for the inference attack, for any error α , we need the distribution of $L(x)$ when x is drawn from the pool and when x is drawn from the population. Estimating the exact distribution of $L(x)$ is a hard problem. Our approach is to approximate the distributions of $L(x)$, through computing its moments $E(L^k)$, $k > 0$. To approximate the distribution using its moments, we use an established statistical principle for fitting a distribution with known moments: the maximum-entropy principle. This principle states that the probability distribution which best represents the current state of knowledge is the one with largest entropy [12, 13].

To simplify the computation of the moments, we take advantage of the Bayesian decomposition to split this $L(x)$ as sum of simpler terms, one term for each attribute X_i . We start by expanding (5) to give the following expression for $L(x)$:

$$\begin{aligned} L(x) &= \log \left(\frac{\Pr[x; \langle G, \theta \rangle]}{\Pr[x; \langle G, \hat{\theta} \rangle]} \right) \\ &= \log \left(\frac{\prod_{i=1}^m \Pr[X_i | Pa_{X_i}^G; \theta]}{\prod_{i=1}^m \Pr[X_i | Pa_{X_i}^G; \hat{\theta}]} \right) \\ &= \sum_{i=1}^m \log \left(\frac{\Pr[X_i | Pa_{X_i}^G; \theta]}{\Pr[X_i | Pa_{X_i}^G; \hat{\theta}]} \right) \end{aligned} \quad (7)$$

where the X_i are the attributes of the data point x , which is now a random variable as it is drawn from the pool (or population), as just mentioned. We define L_i as the contribution of attribute X_i to the likelihood ratio L . Hence the value of L_i can be calculated as:

$$L_i = \log \left(\frac{\Pr[X_i | Pa_{X_i}^G; \theta]}{\Pr[X_i | Pa_{X_i}^G; \hat{\theta}]} \right) \quad (8)$$

We calculate the first two moments of $L(x)$ for our approximation. The mean and variance of $L(x)$ are $\mu_0 = \frac{C}{2n}$, $\sigma_0^2 = \frac{C}{n}$ under the null hypothesis and $\mu_1 = -\frac{C}{2n}$, $\sigma_1^2 = \frac{C}{n}$ under the alternative hypothesis (see proof in Section 5.2). For a known mean μ and

variance σ^2 , the max-entropy distribution that matches the target distribution is a Gaussian $N(\mu, \sigma^2)$. In evaluation section 6.2, we show that approximating the distribution of $L(x)$ using just its first two moments sufficient to calculate accurate bounds on the attack power. We show this by comparing our theoretical bound with the empirically observed maximum power for any error.

Given this approximation, and the computed mean and variance, the relationship between power β , and error α is

$$\mu_0 - z_\alpha \sigma_0 = \mu_1 - z_\beta \sigma_1 \quad (9)$$

where z_s is the quantile at level $1 - s$, $0 < s < 1$ of the standard normal distribution. This equation can be derived by equating quantiles at level β , α in the pool and population distribution respectively.

Substituting $\mu_0, \sigma_0, \mu_1, \sigma_1$ into (9), we derive the main result. \square

We observe that the centers (means) of $L(x)$ under the null and alternative hypotheses are separated by a distance of $\frac{C}{n}$. The overlap between the distributions is determined by variance of the statistic, and the amount of the overlap between the two distributions determines the power $\beta = \Pr_{pool}\{L(x) \leq F^{-1}(\alpha)\}$ for any error α .

Our result generalizes that of Sankararaman et al. [20] on releasing independent marginals. In their case, the released graph has no edges and nodes are binary variables. The complexity of such a graph is equal to the number of nodes m . Hence, for independent marginals we recover Sankararaman et al's relation:

$$z_\alpha + z_{1-\beta} = \sqrt{\frac{m}{n}}. \quad (10)$$

5.1 Insights on power, error, complexity and pool size

The first insight from Theorem 1 is that, for a constant complexity C and pool size n , the attacker cannot simultaneously improve the error and the power. Decreasing the error means increasing the threshold, which would necessarily decrease the power.

Secondly, we can observe and quantify the effect of releasing a more complex model. Releasing more parameters helps the attacker, and we also see that e.g. quadrupling $C(G)$ would double the sum $z_\alpha + z_{1-\beta}$, thus reducing the error or increasing the power or both. The amount of improvement depends on how large the sum already is and there are diminishing returns.

In contrast, increasing the pool size n has the opposite effect to increasing C : the attack performance becomes worse. This makes sense, as a larger pool is more similar to (has more overlap with) the population, so it is more difficult for the attacker to distinguish between them.

It is also possible to see whether a heuristic attack can be improved by comparing its error and power to the ones implied by the main theorem for a given complexity and pool size. From the heuristic attack's error and power, we can compute the corresponding Standard Normal quantiles and compare their sum to $\sqrt{\frac{C(G)}{n}}$. If the sum is far from the bound, then the attack can be improved.

From a defender's point of view, we can quantify the maximum leakage associated with releasing various models **without** having to train each model and **without** having to perform any attack. We can reason about the ultimate/maximum power of the attacker, e.g.

one with perfect knowledge about the population, so as to guide our choice of a model to release.

The bound is independent of the exact values of the data in the pool and depends on the data only via the parameter values of the model. It depends only on the metadata of the model: pool size n , number of attributes m and model structure G . This implies that the analysis is robust to varying the details of the dataset, but it is expressive enough to capture and resolve questions like the following:

- Which one of many model structures to use for the released model to minimize leakage?
- What is the additional leakage caused by releasing one more attribute for each data point in the pool?
- How do the dependencies among a certain group of attributes affect the leakage?
- How exactly does the pool size affect leakage? E.g. if we double the pool size, will that halve the leakage because the released model now is trained on twice as many data points?

5.2 Derivation of mean and variance of the likelihood ratio

We now compute the mean and variance of $L(x)$ under the two hypotheses. We sketch the proof for the mean $E(L)$ under the population hypothesis, followed by the variance $\text{Var}(L)$. Similar calculations apply for the pool hypothesis.

Let the target x have the feature vector (x_1, x_2, \dots, x_m) , and let us assume, for now, that all attributes are binary: $x_i \in \{0, 1\}$, $i = 1, \dots, m$. In Appendix D we generalize to attributes that can take more than two values. We can take advantage of the Bayesian network decomposition to write the log-likelihood ratio for x as follows:

$$\begin{aligned} L(x) &= \log \left[\frac{\Pr(x; \langle G, \theta \rangle)}{\Pr(x; \langle G, \hat{\theta} \rangle)} \right] \\ &= \sum_{i=1}^m L_i \end{aligned} \quad (11)$$

where L_i is the contribution of X_i to the likelihood ratio, as defined in (8):

$$\begin{aligned} L_i &= \log \left(\frac{\Pr[X_i | Pa_{X_i}^G; \theta]}{\Pr[X_i | Pa_{X_i}^G; \hat{\theta}]} \right) \\ &= \sum_{v \in V(Pa_{X_i}^G)} 1_{\{Pa_{X_i}^G = v\}} \underbrace{\left(x_i \log \frac{p_i^v}{\hat{p}_i^v} + (1 - x_i) \log \frac{1 - p_i^v}{1 - \hat{p}_i^v} \right)}_{L_i^v} \\ &= \sum_{v \in V(Pa_{X_i}^G)} 1_{\{Pa_{X_i}^G = v\}} L_i^v \end{aligned} \quad (12)$$

where $p_i^v = \Pr\{X_i = 1 | Pa_{X_i}^G = v; \theta\}$, and similarly $\hat{p}_i^v = \Pr\{X_i = 1 | Pa_{X_i}^G = v; \hat{\theta}\}$. The notation $1_{\{Pa_{X_i}^G = v\}}$ is an indicator variable for a particular assignment of values to the parent nodes of X_i , i.e. $1_{\{Pa_{X_i}^G = v\}} = 1$ if $Pa_{X_i}^G = v$ and 0 otherwise. The sum ranges over $2^{|Pa_{X_i}^G|}$ terms L_i^v , one for each element of $V(Pa_{X_i}^G)$.

The parameters θ and $\hat{\theta}$ are estimated from data (reference population and pool, respectively). By the central limit theorem, the distribution of such an estimate converges to a Gaussian around the mean value of the estimate as the number of data samples increases. In our derivations of the mean and variance, we use this approximation in (20) and (21). By the Berry-Esseen theorem [4, 8], the rate of convergence to the Gaussian is $O(\frac{1}{\sqrt{n}})$ if the third moment of the random variable being sampled is finite. In our case this condition is true, because each random variable can only take a finite number of possible finite values.

We compute the mean and variance of $L(x)$ as follows:

$$E_{pop}(L) = \frac{C}{2n} + O(Cn^{-2}) \quad (13a)$$

$$E_{pool}(L) = -\frac{C}{2n} + O(Cn^{-2}) \quad (13b)$$

$$\text{Var}_{pop}(L) = \frac{C}{n} + O(C^2n^{-2}) \quad (13c)$$

$$\text{Var}_{pool}(L) = \frac{C}{n} + O(C^2n^{-2}). \quad (13d)$$

PROOF SKETCH - MEAN UNDER H_{OUT}. The mean $E_{pop}(L)$ can be computed as follows:

$$\begin{aligned} E_{pop}(L) &= \sum_{i=1}^m E_{pop}(L_i) \\ &= \sum_{i=1}^m \sum_v E_{pop}(1_{\{Pa_{X_i}^G=v\}} L_i^v) \end{aligned} \quad (14)$$

Using approximation (22) in Appendix Section B, we compute $E_{pop}(1_{\{Pa_{X_i}^G=v\}} L_i^v) \approx \frac{1}{2n} + O(n^{-2})$. Since the total number of L_i^v parameters is $C = \sum_{i=1}^m 2^{|Pa_{X_i}^G|}$, we conclude that

$$E_{pop}(L) = \frac{C}{2n} + O(Cn^{-2}). \quad (15)$$

□

PROOF SKETCH - VARIANCE UNDER H_{OUT}. By definition,

$$\text{Var}_{pop}(L) = E_{pop}[L^2] - (E_{pop}[L])^2. \quad (16)$$

The latter term $(E_{pop}[L])^2$ is the square of the mean, which we compute in (15). The former term $E_{pop}[L^2]$ decomposes as follows:

$$E_{pop}[L^2] = \sum_{i=1}^m E_{pop}[L_i^2] + 2 \sum_{1 \leq i < j \leq m} E_{pop}[L_i L_j] \quad (17)$$

We compute $E_{pop}[L_i^2]$ by expanding $E_{pop}[(\sum_v 1_{\{Pa_{X_i}^G=v\}} L_i^v)^2]$. Then, approximation (32) in Appendix C gives us that each square term $E_{pop}[(1_{\{Pa_{X_i}^G=v\}} L_i^v)^2]$ is approximately equal to $\frac{1}{n} |V(Pa_{X_i}^G)|$. As for the product terms in the expansion, each term multiplies two different indicator variables $1_{\{Pa_{X_i}^G=v\}}$ and $1_{\{Pa_{X_i}^G=v'\}}$ with $v \neq v'$. Because at most one of the two is equal to 1, all product terms will be zero. Hence $E_{pop}[L_i^2] = 2^{|Pa_{X_i}^G|} \times \frac{1}{n}$.

The number of joint terms $E_{pop}[L_i L_j]$ is $O(C^2)$. From the approximation in Appendix Section C.1 for $E_{pop}[L_i L_j]$, each of these

terms is equal to $\frac{1}{4n^2}$ with error term $O(n^{-2})$. Hence, the value of $E_{pop}[L^2]$ is

$$E_{pop}[L^2] = \frac{C}{n} + \frac{C^2}{4n^2} + O(C^2n^{-2}). \quad (18)$$

We conclude that the variance is

$$\begin{aligned} \text{Var}_{pop}(L) &= E_{pop}[L^2] - (E_{pop}[L])^2 \\ &= \frac{C}{n} + \frac{C^2}{4n^2} + O(C^2n^{-2}) - \left(\frac{C}{2n} + O(Cn^{-2}) \right)^2 \\ &= \frac{C}{n} + O(C^2n^{-2}) \end{aligned} \quad (19)$$

□

Although we haven't provided the calculation here, it is possible to calculate the exact value of the $O(C^2n^{-2})$ term from the released model. As a simple example, in appendix E, we calculate the exact value of this $O(C^2n^{-2})$ term, when the released model is a Naive Bayes model.

6 EXPERIMENTS

We distinguish three different methods for performing and evaluating the attack below:

- (1) **Theoretical:** Given a false positive rate and released model structure G , we use our main result (Theorem 1) to calculate the power, error, and AUC.
- (2) **Empirical:** In empirical analysis we vary the threshold from $-\infty$ to $+\infty$ and calculate the power at each value of false positive rate. This is the maximum possible power that can be achieved. Hence we use the power and AUC values calculated here to compare with the bound presented in Theorem 1.
- (3) **Attack:** The adversary has access to some reference population. For a given false positive rate, the adversary chooses the threshold based on the likelihood ratio on the reference population data. The attacker then runs the LR test tracing attack.

6.1 Data Sets

A summary of all the data sets which are used in our experiments is provided in Table 2.

Location: This is a binary data set containing the Foursquare location check-ins by individuals in Bangkok [21]. Each record corresponds to an individual and consists of binary attributes reflecting visits to different locations.

Purchase: This is a binary data set containing information about individuals and their purchases [21]. Each record corresponds to an individual and each attribute represents a product. A value of 1 at attribute j means that the individual purchased the product corresponding to attribute j .

Genome: OpenSNP is an open source data sharing website, where people can share their genomic data test results¹. We obtained the data provided by OpenSNP and considered only the individuals sequenced by 23andme. We randomly selected 1000 SNPs on chromosome 1. Individuals with more than 2 missing values were filtered out. After this pre-processing, we were left with 2497 individuals and 1000 SNPs for each individual. We learn a

¹<https://opensnp.org/snps>

Data Set	# Attributes	Original Size	Augmented Dataset Size
Location	446	5010	30000
Purchase	600	30000	30000
Genome	1000	2497	10000

Table 2: Summary of Datasets used: For Location and Genome data, we augment the original dataset with synthetic data using the data synthesis method in Section 2.3, based on a Bayesian network with $\eta = 3$ (see Section 2.1). We use the full augmented set as the general population.

Data set	η	No. of Nodes	No. of Edges	Complexity
Location	0	446	0	446
Location	1	446	343	789
Location	2	446	566	1222
Location	3	446	757	1905
Purchase	0	600	0	600
Purchase	1	600	496	1096
Purchase	2	600	941	1942
Purchase	3	600	1358	3431
Genome	0	1000	0	1000
Genome	1	1000	729	1729
Genome	2	1000	1244	2706
Genome	3	1000	1712	4323

Table 3: Model structures we learned on different datasets, with different complexities. The structure learning is done on all the available data. The variable η represents maximum number of parents a node can have in the graph. These structures are used as G in the experiments.

Bayesian network of complexity 4323 on the real data and use it to generate synthetic data. After adding synthetic data, we have a total of 10000 individuals in the dataset.

Bayesian Networks have been used to model genome sequences in [1], [22]. We use a similar approach to model the SNPs as a Bayesian Network. Since humans are diploid, at each position we have 2 bases i.e. 3 possible values. While releasing graphical models constructed from genomic data, we only estimate the Minor and Major Allele Frequencies. To calculate the probability of any combination, we assume independence and compute it as the product of Allele Frequencies.

In all the experiments, the pool and reference population are sampled independently from the total population. To evaluate the attack, all the available samples from general population are used to compute power and false positives. The pool size and reference population size for experiments with the Location and Purchase datasets are 3000 and 15000 respectively. The pool size and reference population size for experiments with the Genome dataset are 1000 and 5000 respectively. We perform each experiment with 50 different and independent splits of pool and reference population and report the average statistics.

Complexity	AUC (Empirical)	AUC (Theoretical)
446	0.5928	0.6074
789	0.6337	0.6416
1222	0.6655	0.6741
1905	0.6998	0.7134

Table 4: Area Under Curve for different graphical models on Location data: Area under curve increases as the model becomes more complex.

6.2 Validity of theoretical bounds on power

We now compare the observed power of tracing attack with the bounds provided in Theorem 1. In Figure 1 (columns 2, 3), we compare the observed power with the theoretical bound. Columns 2 and 3 correspond to releasing Bayesian Networks learned with $\eta = 0$ and $\eta = 3$ respectively.

For models with $\eta = 0$ (column 2), we can see that the observed power is much less than the theoretical bound, compared to the case of $\eta = 3$ (column 3). For Location data, the empirical power exactly matches the bound for both $\eta = 0$ and $\eta = 3$. The power of the attack is very small on location data because of the small number of attributes (446) and the comparatively large pool size (3000).

When the released model does not capture all the dependencies among attributes in data (under fitted), estimation errors of parameters in released graphical model become correlated. This effectively reduces the amount of information available to perform membership inference. When $\eta = 0$, the model cannot capture any dependency in the data. Hence, the difference between the observed power and the bound will be larger, which can be seen in Figure 1 (column 2). As η increases, the model captures more of the dependencies present in the data. When $\eta = 3$, as shown in Figure 1 (column 3), the observed power is very close to the theoretical bound. **The observed power of tracing attack becomes closer to the theoretical bound as the graphical model becomes more complex.**

6.3 Effect of model complexity on power

In this subsection, we discuss how the complexity of released graphical model affects the power of tracing attack. Figure 1 (column 1) shows the power of tracing attack when models of various complexities are released. We can observe that, with increasing value of η , the power of attack increases.

The Area Under Curve of the ROC plot helps quantify the increase in power with complexity in a better way. Tables 4, 5, 6 give the AUC values of attack on Location, Purchase and Genomes data respectively. The AUC values are comparatively smaller for the purchase data set compared to that of the Genomes dataset. This is because, in case of purchase we only have 600 attributes for a pool size of 3000. In case of Genomic data, we have 1000 attributes for a pool size of 1000. Even then, as shown in Table 5 on purchase data, if a bayesian network with $\eta = 3$ is released, we can achieve an AUC value of approximately 0.75, compared to 0.57 when only marginals

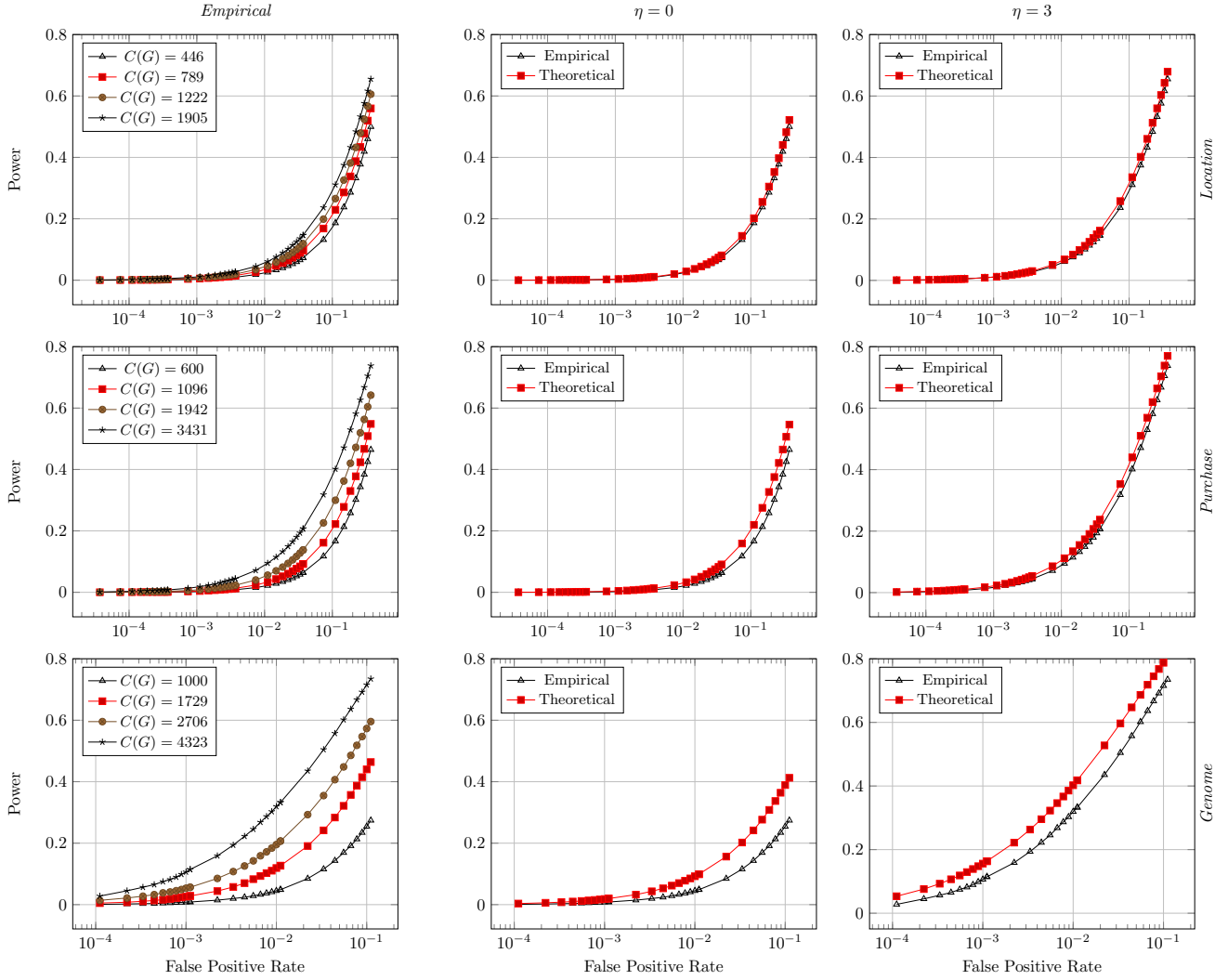


Figure 1: Power of Attack on Real world data: The effect of model complexity on the power of the attack is shown in the first column. When graphical models of increasing complexity are released, the power of attack increases, as we have more parameters that leak information. In the second and third columns, we compare the observed powers with their corresponding theoretical bounds. When the model is underfitted, the power achieved will be smaller than the theoretical bound (second column). As the released model gets closer to the generator distribution, the observed power gets closer to the bound.

are released. We can clearly conclude that with increasing value of η , the power of tracing attack increases.

When learning the structure of Bayesian Network, higher values of η result in graphical models with high complexity. Exact values of complexity for the corresponding η are shown in Table 3. The complexity of a graphical model represents the number of independent parameters in the model. Each of these parameters is learned from individuals in the pool. When Bayesian Networks of high complexity are learned from limited data, parameters of network overfit the data more and hence can leak more information about membership. This additional leakage increases the power of the tracing attack. **The higher the complexity of the released model, the higher the power of the tracing attack.**

Complexity	AUC (Empirical)	AUC (Theoretical)
600	0.5700	0.6241
1096	0.6266	0.6655
1942	0.6886	0.7153
3431	0.7541	0.7752

Table 5: Area Under Curve for different graphical models on Purchase data: Area under curve increases as model becomes more complex.

Complexity	AUC (Empirical)	AUC (Theoretical)
1000	0.6729	0.7602
1729	0.7875	0.8238
2706	0.8495	0.8776
4323	0.9058	0.9292

Table 6: Area Under Curve for different graphical models on Genome data: As the released model becomes more complex, Area under curve increases and gets closer to theoretical bound.

6.4 Effect of using complex model as population model

In this subsection, we present the effect of population model choice on the power of tracing attack. Specifically, we study the effect of using models that are more complex than the released model as population model. The adversary can choose to use either the released graphical model structure G or a complex model structure G_{pop} as population model structure. Figure 2 compares the power of attack for both the choices of population model. The parameters of a graphical model $\langle G, \theta \rangle$ with $\eta = 1$ are learned on the pool data and released. The adversary has access to a complex and better representative model $\langle G_{pop}, \theta \rangle$ that was learned with $\eta = 3$. The power of the attack is higher when the released model structure is used as population model structure. The knowledge about additional dependencies that are not present in the released graph structure cannot increase the power of adversary. **The optimal strategy for adversary is to use the released model structure as population model structure.**

6.5 Effect of releasing statistically insignificant edges

We now analyze the effect on the power of attack of releasing edges (conditional probabilities) that are statistically insignificant. To perform this evaluation, we consider the case where the structure of released model is not learned from data but generated in a random way.

Figure 3 compares the power of the attack when two different models of almost equal complexity are released. The structure of first model is generated by randomly adding edges and the structure of second model is learned from data. Adversary uses the released model as the population model to calculate the LR statistic and perform tracing attack. We can observe that the power of the attack in both the cases is similar.

The edges that are generated randomly might not be statistically significant, but they leak about membership. In the LR Test for tracing attack, we rely on the difference between probability distributions for pool and population. Adding a statistically insignificant edge gives similar probability distributions for all configurations of the parent. Although the conditional probabilities are similar, their values will be different for pool and population and hence they will leak about membership. **Statistically insignificant edges leak as much information about membership as significant edges.**

6.6 Optimality of the theoretical threshold

In Figure 4, we compare theoretical thresholds for certain false positive rates with their corresponding values estimated using the reference population. When $\eta = 0$ (row 1), we observe that the theoretical threshold values are much higher than the estimated values. When $\eta = 3$ (row 2), the observed thresholds are closer to the estimated values.

When $\eta = 0$, the parameter estimation errors are correlated, which reduces the amount of information leakage. The adversary, when using the theoretical threshold, overestimates the amount of leakage (power) and hence chooses a higher threshold. When $\eta = 3$, the released model captures most of the dependencies among attributes in the data. Hence the observed threshold will be closer to the theoretical threshold values. **From the adversary’s perspective, the theoretical threshold value is sub-optimal when the released model is underfitted (loss of utility).**

7 RELATED WORK

Tracing Attacks: Homer et al. [10] developed a statistical test based on likelihood ratio for inferring the presence of a genome sequence, given the statistics (Allele frequencies). Sankararaman et al. [20] extend this work and provide tight bounds on the power of tracing attack for any adversary. The test statistic in [20] is based on likelihood ratio. This was further extended for continuous Gaussian variables (Micro RNA) data in [3].

Dwork et al. [7] take a different approach and provide a generic framework for tracing attacks based on distance metric, when independent statistics are released. [7] provides bounds on power of adversary with different levels of background knowledge ranging from one reference population sample to infinite reference population. In all of [3, 7, 10, 20] the released statistics are assumed to be independent, whereas our work address the case of releasing dependent statistics.

[11] perform tracing attacks when regression coefficients from quantitative phenotypes are released, based on a correlation statistic. Theoretical bound on maximum power achievable by the adversary was provided by calculating the distribution of test statistic for individuals in pool and individuals out of pool.

Shokri et al. [21] perform membership inference attacks against black box machine learning models. The adversary in [21] constructs *shadow models* that mimic the behaviour of target model. The attack step is also a machine learning model, which is trained on data from the shadow models. [19] perform membership inference on aggregate location data by formulating it as distinguishing game. These works provide empirical analysis of tracing attack on complex models. Often this performance depends on the training data. We present a theoretical bound that is independent of the training data.

[23] study the connection of privacy loss to overfitting and influence of a point. Their theoretical analysis suggests that overfitting is sufficient for membership inference attacks to be possible but it is not a necessary condition.

Other Privacy Attacks on PGMs: [6] provides a polynomial time algorithm to reconstruct databases from noisy statistics. [2] perform inference attacks i.e. reconstruction of hidden attributes against genomic data by modeling it as a Markov Chain.

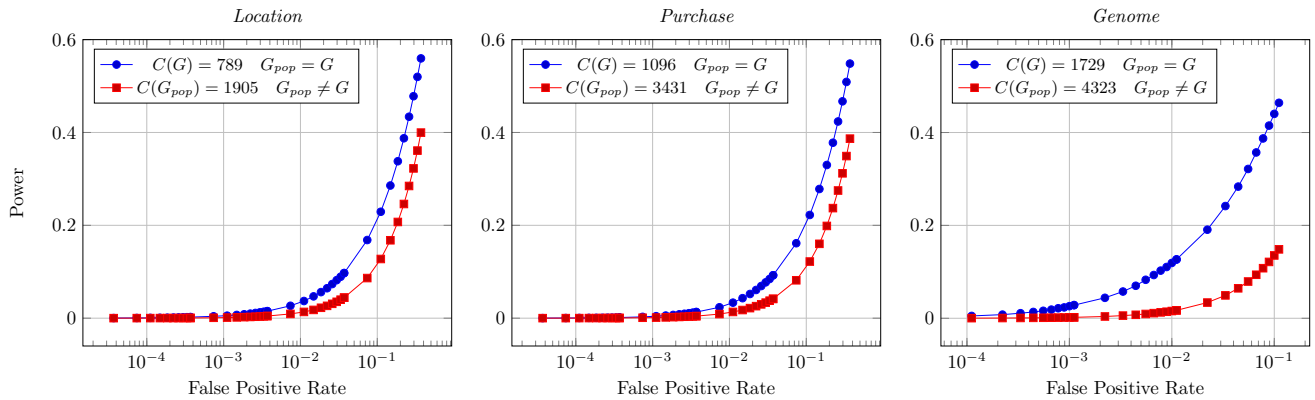


Figure 2: Effect of using generative model as population model: The parameters of a graphical model $\langle G, \hat{\theta} \rangle$ with $\eta = 1$ are learned on the pool data and the model is released. The adversary has access to a better generative model $\langle G_{pop}, \theta \rangle$ with $(\eta = 3)$. Plot compares effect of using the better model as population model instead of released model, on power of attack. We can see that the power of attack reduces when the population model is more complex than released model. This shows that knowledge about additional statistics/dependencies in the data that are not present in the released graphical model, cannot increase the power of attack. The optimal strategy for adversary is to use the released graph structure as population graph structure.

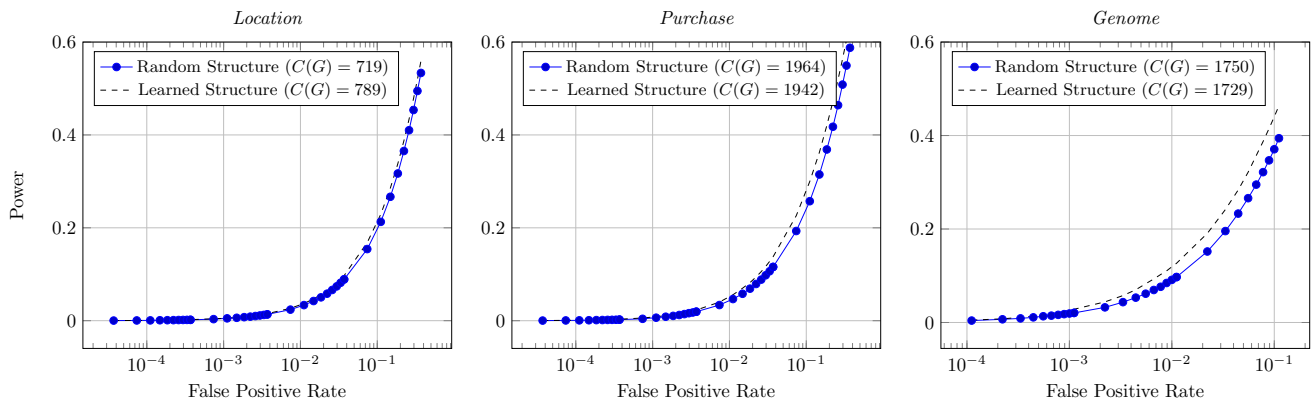


Figure 3: Effect of Releasing Graphical Models with Random Edges: Here we compare the power of attack, when two models of similar complexity learned on the dataset are released but structure of one model is learned from data and the structure of other is generated randomly. We can see that for close values of C , the power of attack is almost same for both the models. This shows that statistically insignificant edges leak as much information about membership, as that of significant edges.

Defenses: Differential Privacy has been accepted as the defacto standard notion of privacy. Zhang et al. [24] learn a Bayesian Network in differentially private way and then use a noisy version of it to generate synthetic data. [5] proposes a mechanism to generate synthetic data that is statistically similar to the given input data set. By definition, differential privacy decreases the power of tracing attack. [16] takes a different approach and train a neural network with membership privacy by modeling the training process a min-max privacy game.

Applications of PGM: [1] uses Bayesian Networks to addresses the problem of classifying hematological malignancies along with co-expression networks. The Bayesian Network was learned on gene expression data. Certain dependencies in this learned Bayesian

Network were made public through the paper. [22] discuss the applicability of Bayesian Networks to model the effect of environment and genes on diseases. A Bayesian Network model was used to model bladder cancer study data in [22]. [14] shows the applicability of Bayesian Networks as intelligent tutoring systems by modeling students. The increasing use of graphical models in sensitive domains, raises the significance of our privacy analysis on releasing high dimension models learned on private data.

8 CONCLUSIONS

We provide a theoretical framework for tracing attacks to close the existing gap between theoretical analysis for simple released models (independent attributes of data samples) and experimental demonstrations for correlated attributes of data samples. Our

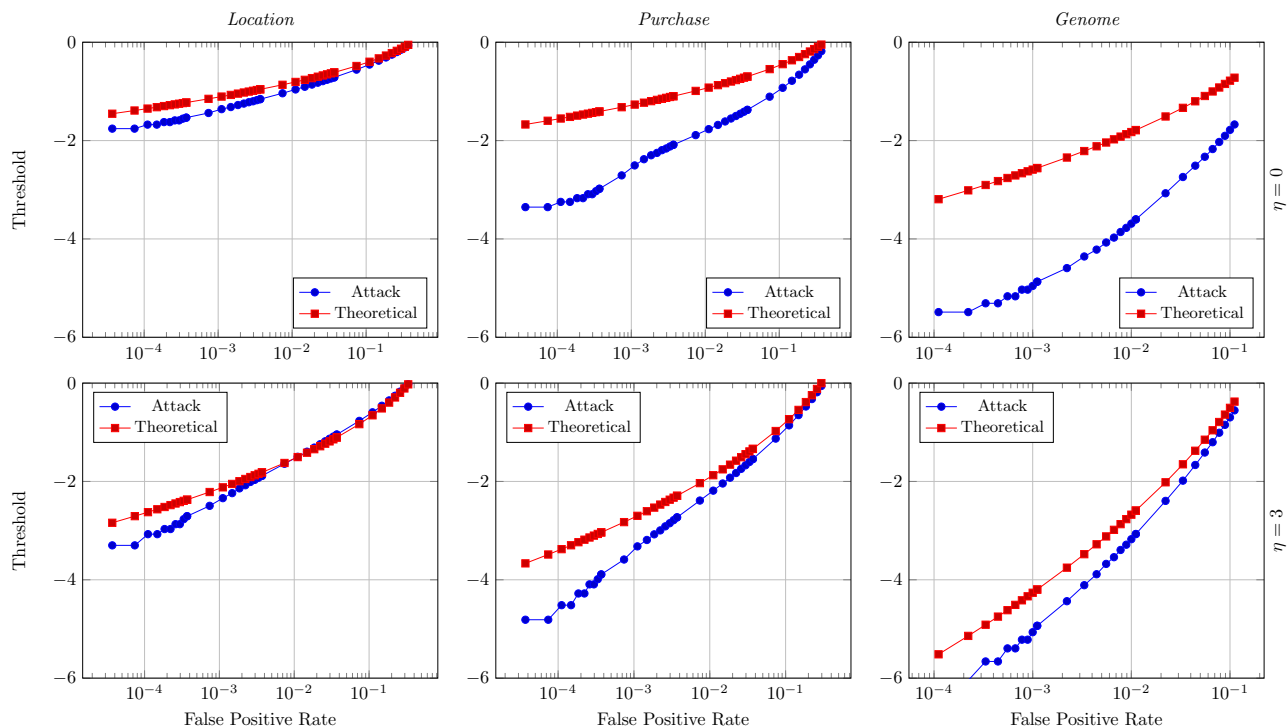


Figure 4: Effect of releasing underfitted models on threshold selection: This plot compares the threshold values estimated by the adversary using reference population at different false positive rates with their corresponding theoretical values. The label Attack indicates that the threshold is estimated by the adversary using reference population. We observe that for underfit models ($\eta = 0$) (first row), the threshold value estimated from the reference population is way less than the corresponding theoretical value. As the model gets closer to the generator distribution ($\eta = 3$) (second row), the estimated threshold values get closer to the theoretical values.

framework quantifies the maximum attack performance measured with the error (false positive rate) and power (true positive rate) of a likelihood-ratio test in the context of probabilistic graphical models. We experimentally validate and complement our theoretical results using sensitive datasets - location check-ins, purchase history, genomic data.

REFERENCES

- [1] Rupesh Agrahari, Amir Foroushani, T Roderick Docking, Linda Chang, Gerben Duns, Monika Hudoba, Aly Karsan, and Habil Zare. 2018. Applications of Bayesian network models in predicting types of hematological malignancies. *Scientific reports* 8, 1 (2018), 6951.
- [2] Erman Ayday and Mathias Humbert. 2017. Inference attacks against kin genomic privacy. *IEEE Security & Privacy* 5 (2017), 29–37.
- [3] Michael Backes, Pascal Berrang, Mathias Humbert, and Praveen Manoharan. 2016. Membership privacy in MicroRNA-based studies. In *Proceedings of the 2016 ACM SIGSAC Conference on Computer and Communications Security*. ACM, 319–330.
- [4] Andrew C Berry. 1941. The accuracy of the Gaussian approximation to the sum of independent variates. *Transactions of the american mathematical society* 49, 1 (1941), 122–136.
- [5] Vincent Bindshaedler, Reza Shokri, and Carl A Gunter. 2017. Plausible deniability for privacy-preserving data synthesis. *Proceedings of the VLDB Endowment* 10, 5 (2017), 481–492.
- [6] Irit Dinur and Kobbi Nissim. 2003. Revealing information while preserving privacy. In *Proceedings of the twenty-second ACM SIGMOD-SIGACT-SIGART symposium on Principles of database systems*. ACM, 202–210.
- [7] Cynthia Dwork, Adam Smith, Thomas Steinke, Jonathan Ullman, and Salil Vadhan. 2015. Robust traceability from trace amounts. In *Foundations of Computer Science (FOCS), 2015 IEEE 56th Annual Symposium on*. IEEE, 650–669.
- [8] Carl-Gustav Esseen. 1942. On the Liapounoff limit of error in the theory of probability. *Arkiv för matematik, astronomi och fysik* (1942).
- [9] Mark Andrew Hall. 1999. Correlation-based feature selection for machine learning. (1999).
- [10] Nils Homer, Szabolcs Szelinger, Margot Redman, David Duggan, Waibhav Tembe, Jill Muehling, John V Pearson, Dietrich A Stephan, Stanley F Nelson, and David W Craig. 2008. Resolving individuals contributing trace amounts of DNA to highly complex mixtures using high-density SNP genotyping microarrays. *PLoS genetics* 4, 8 (2008), e1000167.
- [11] Hae Kyung Im, Eric R Gamazon, Dan L Nicolae, and Nancy J Cox. 2012. On sharing quantitative trait GWAS results in an era of multiple-omics data and the limits of genomic privacy. *The American Journal of Human Genetics* 90, 4 (2012), 591–598.
- [12] Edwin T Jaynes. 1957. Information theory and statistical mechanics. *Physical review* 106, 4 (1957), 620.
- [13] Edwin T Jaynes. 1957. Information theory and statistical mechanics. II. *Physical review* 108, 2 (1957), 171.
- [14] Tanja Käser, Severin Klingler, Alexander G Schwing, and Markus Gross. 2017. Dynamic Bayesian networks for student modeling. *IEEE Transactions on Learning Technologies* 10, 4 (2017), 450–462.
- [15] Daphne Koller, Nir Friedman, and Francis Bach. 2009. *Probabilistic graphical models: principles and techniques*. MIT press.
- [16] Milad Nasr, Reza Shokri, and Amir Houmansadr. 2018. Machine Learning with Membership Privacy using Adversarial Regularization. In *Proceedings of the 2018 ACM SIGSAC Conference on Computer and Communications Security*. ACM, 634–646.
- [17] M. Nasr, R. Shokri, and A. Houmansadr. 2019. Comprehensive Privacy Analysis of Deep Learning: Passive and Active White-box Inference Attacks against Centralized and Federated Learning. In *IEEE Symposium on Security and Privacy (SP)*. 1022–1036. <https://doi.org/10.1109/SP.2019.00065>

- [18] Jerzy Neyman and Egon Sharpe Pearson. 1933. IX. On the problem of the most efficient tests of statistical hypotheses. *Philosophical Transactions of the Royal Society of London. Series A, Containing Papers of a Mathematical or Physical Character* 231, 694-706 (1933), 289–337.
- [19] Apostolos Pyrgelis, Carmela Troncoso, and Emiliano De Cristofaro. 2017. Knock Knock, Who's There? Membership Inference on Aggregate Location Data. *arXiv preprint arXiv:1708.06145* (2017).
- [20] Sriram Sankararaman, Guillaume Obozinski, Michael I Jordan, and Eran Halperin. 2009. Genomic privacy and limits of individual detection in a pool. *Nature genetics* 41, 9 (2009), 965.
- [21] Reza Shokri, Marco Stronati, Congzheng Song, and Vitaly Shmatikov. 2017. Membership inference attacks against machine learning models. In *Security and Privacy (SP), 2017 IEEE Symposium on*. IEEE, 3–18.
- [22] Chengwei Su, Angeline Andrew, Margaret R Karagas, and Mark E Borsuk. 2013. Using Bayesian networks to discover relations between genes, environment, and disease. *BioData mining* 6, 1 (2013), 6.
- [23] Samuel Yeom, Irene Giacomelli, Matt Fredrikson, and Somesh Jha. 2018. Privacy risk in machine learning: Analyzing the connection to overfitting. In *2018 IEEE 31st Computer Security Foundations Symposium (CSF)*. IEEE, 268–282.
- [24] Jun Zhang, Graham Cormode, Cecilia M Procopiuc, Divesh Srivastava, and Xiaokui Xiao. 2017. Privbayes: Private data release via bayesian networks. *ACM Transactions on Database Systems (TODS)* 42, 4 (2017), 25.

A NUMBER OF SAMPLES FOR ESTIMATING CONDITIONAL PROBABILITIES

We use \hat{p}_i^v to denote the estimated conditional probability that $X_i = 1$, given that the values of the activator variables are $Pa_{X_i}^G = v$. The number of samples n_i^v used to compute \hat{p}_i^v are approximately Gaussian around np_v (n is the pool size, and p_v is the probability of $Pa_{X_i}^G = v$ in the general population):

$$n_i^v \approx np_v + \sqrt{np_v(1-p_v)}Z_1, \quad (20)$$

where Z_1 is a standard Gaussian random variable. In parallel, the value of \hat{p}_i^v is also approximately Gaussian around the true value p_i^v :

$$\hat{p}_i^v \approx p_i^v + \sqrt{\frac{p_i^v(1-p_i^v)}{n_i^v}}Z_2, \quad (21)$$

where Z_2 is a standard Gaussian random variable.

Using these two approximations, we now prove the results required for derivation of LR statistic mean and variance.

B APPROXIMATION FOR MEAN DERIVATION

As explained in section 5.2, to compute the mean of the likelihood ratio we need the average contribution of each L_i^v i.e. value of $E_{pop}[1_{\{Pa_{X_i}^G=v\}}L_i^v]$. Here we prove that $E_{pop}[1_{\{Pa_{X_i}^G=v\}}L_i^v]$, when the expectation is over population is approximately equal to $\frac{1}{2n}$. When expectation is over pool, the derivation steps are similar and the value is $-\frac{1}{2n}$.

LEMMA 1. *We will prove the following result:*

$$E_{pop}[1_{\{Pa_{X_i}^G=v\}}L_i^v] \approx \frac{1}{2n} \left(1 + \frac{1-p_v}{np_v}\right) \quad (22)$$

PROOF. We first observe that

$$\begin{aligned} E_{pop}[1_{\{Pa_{X_i}^G=v\}}L_i^v] &= E_{\hat{p}_i^v} \left[E_x \left[1_{\{Pa_{X_i}^G=v\}}L_i^v \mid \hat{p}_i^v \right] \right] \\ &= p_v E_{\hat{p}_i^v} \left[p_i^v \log \frac{p_i^v}{\hat{p}_i^v} + (1-p_i^v) \log \frac{1-p_i^v}{1-\hat{p}_i^v} \right], \end{aligned}$$

and now all we need to show is that

$$\begin{aligned} E_{Z_1, Z_2} \left[p_i^v \log \frac{p_i^v}{\hat{p}_i^v} + (1-p_i^v) \log \frac{1-p_i^v}{1-\hat{p}_i^v} \right] \\ \approx \frac{1}{2np_v} \left(1 + \frac{1-p_v}{np_v}\right) \end{aligned} \quad (23)$$

We approximate \hat{p}_i^v with (21) and we use the Taylor expansion of $\log(1+x) \approx x - \frac{1}{2}x^2$:

$$\begin{aligned} p_i^v \log \frac{p_i^v}{\hat{p}_i^v} &\approx -p_i^v \log \frac{p_i^v + \sqrt{\frac{p_i^v(1-p_i^v)}{n_i^v}}Z_2}{p_i^v} \\ &= -p_i^v \log \left(1 + \sqrt{\frac{1-p_i^v}{n_i^v p_i^v}}Z_2\right) \\ &\approx -p_i^v \left(\sqrt{\frac{1-p_i^v}{n_i^v p_i^v}}Z_2 - \frac{1-p_i^v}{2n_i^v p_i^v}Z_2^2 \right) \\ &= -\sqrt{\frac{p_i^v(1-p_i^v)}{n_i^v}}Z_2 + \frac{1-p_i^v}{2n_i^v}Z_2^2 \end{aligned} \quad (24)$$

Similarly,

$$(1-p_i^v) \log \frac{1-p_i^v}{1-\hat{p}_i^v} \approx -\sqrt{\frac{p_i^v(1-p_i^v)}{n_i^v}}Z_2 + \frac{p_i^v}{2n_i^v}Z_2^2 \quad (25)$$

Adding (24) and (25), we have

$$p_i^v \log \frac{p_i^v}{\hat{p}_i^v} + (1-p_i^v) \log \frac{1-p_i^v}{1-\hat{p}_i^v} \approx -2\sqrt{\frac{p_i^v(1-p_i^v)}{n_i^v}}Z_2 + \frac{1}{2n_i^v}Z_2^2 \quad (26)$$

Taking the expectation $E_{Z_2}[\cdot]$, and recalling that $E[Z_2] = 0$ and $E[Z_2^2] = 1$, we have

$$\begin{aligned} E_{Z_1, Z_2} \left[p_i^v \log \frac{p_i^v}{\hat{p}_i^v} + (1-p_i^v) \log \frac{1-p_i^v}{1-\hat{p}_i^v} \right] &= E_{Z_1} [E_{Z_2}[\dots | Z_1]] \\ &\approx E_{Z_1} \left[\frac{1}{2n_i^v} \right] \end{aligned} \quad (27)$$

We now approximate n_i^v with (20) and we use the Taylor expansion of $\frac{1}{1+x} \approx 1 - x + x^2$:

$$\begin{aligned} \frac{1}{2n_i^v} &\approx \frac{1}{2(np_v + \sqrt{np_v(1-p_v)}Z_1)} \\ &= \frac{1}{2np_v} \frac{1}{1 + \sqrt{\frac{1-p_v}{np_v}}Z_1} \\ &\approx \frac{1}{2np_v} \left(1 - \sqrt{\frac{1-p_v}{np_v}}Z_1 + \frac{1-p_v}{np_v}Z_1^2\right) \end{aligned} \quad (28)$$

Taking the expectation $E_{Z_1}[\cdot]$, and recalling that $E[Z_1] = 0$ and $E[Z_1^2] = 1$, we have our final result:

$$\begin{aligned} E_{Z_1, Z_2} \left[p_i^v \log \frac{p_i^v}{\hat{p}_i^v} + (1-p_i^v) \log \frac{1-p_i^v}{1-\hat{p}_i^v} \right] \\ \approx \frac{1}{2np_v} \left(1 + \frac{1-p_v}{np_v}\right) \end{aligned}$$

□

C APPROXIMATION FOR VARIANCE DERIVATION

For calculating the variance of likelihood ratio, we need the expected values of L_i^2 and $L_i L_j$. Here we first prove the below approximation and use it to calculate $E(L_i^2)$ and $E(L_i L_j)$. As explained in section 5.2, using these values of $E(L_i^2)$ and $E(L_i L_j)$ in equation 17 we get the variance of LR statistic.

LEMMA 2. *We will prove the following approximation:*

$$\begin{aligned} & E_{\hat{p}_i^v} \left[p_i^v \left(\log \frac{p_i^v}{\hat{p}_i^v} \right)^2 + (1 - p_i^v) \left(\log \frac{1 - p_i^v}{1 - \hat{p}_i^v} \right)^2 \right] \\ & \approx \frac{1}{np_v} \left(1 + \frac{1 - p_v}{np_v} \right) \end{aligned} \quad (29)$$

PROOF. Using approximation (24)

$$\begin{aligned} & E_{\hat{p}_i^v} \left[p_i^v \left(\log \frac{p_i^v}{\hat{p}_i^v} \right)^2 \right] \approx E_{Z_1, Z_2} \left[\frac{1}{p_i^v} \left(-\sqrt{\frac{p_i^v(1 - p_i^v)}{n_i^v}} Z_2 \right. \right. \\ & \quad \left. \left. + \frac{1 - p_i^v}{2n_i^v} Z_2^2 \right)^2 \right] \\ & = \frac{1}{p_i^v} E_{Z_1, Z_2} \left[\frac{p_i^v(1 - p_i^v)}{n_i^v} Z_2^2 + \left(\frac{1 - p_i^v}{2n_i^v} \right)^2 Z_2^4 \right. \\ & \quad \left. - 2\sqrt{\frac{p_i^v(1 - p_i^v)}{n_i^v}} \frac{1 - p_i^v}{2n_i^v} Z_2^3 \right] \\ & = \frac{1}{p_i^v} E_{Z_1} \left[\frac{p_i^v(1 - p_i^v)}{n_i^v} + 3 \left(\frac{1 - p_i^v}{2n_i^v} \right)^2 \right] \\ & \approx (1 - p_i^v) E_{Z_1} \left[\frac{1}{n_i^v} \right] \\ & \approx (1 - p_i^v) E_{Z_1} \left[\frac{1}{np_v} \left(1 - \sqrt{\frac{1 - p_v}{np_v}} Z_1 + \frac{1 - p_v}{np_v} Z_1^2 \right) \right] \\ & = \frac{1 - p_i^v}{np_v} \left(1 + \frac{1 - p_v}{np_v} \right) \end{aligned} \quad (30)$$

Similar to (30), we have:

$$E_{\hat{p}_i^v} \left[(1 - p_i^v) \left(\log \frac{1 - p_i^v}{1 - \hat{p}_i^v} \right)^2 \right] \approx \frac{p_i^v}{np_v} \left(1 + \frac{1 - p_v}{np_v} \right) \quad (31)$$

The desired result follows. \square

C.1 Approximation of $E_{pop}[L_i^2]$

We approximate $E_{pop}[L_i^2]$ as:

$$\begin{aligned} E_{pop}[L_i^2] & = E_{pop} \left[\left(\sum_v 1_{\{Pa_{X_i}^G = v\}} L_i^v \right)^2 \right] \\ & = E_{\hat{p}_i^v} \left[E \left[\left(\sum_v 1_{\{Pa_{X_i}^G = v\}} L_i^v \right)^2 \middle| \hat{p}_i^v \right] \right] \\ & = \sum_v p_v E_{\hat{p}_i^v} [(L_i^v)^2] \\ & = \sum_v p_v E_{\hat{p}_i^v} \left[p_i^v \left(\log \frac{p_i^v}{\hat{p}_i^v} \right)^2 + (1 - p_i^v) \left(\log \frac{1 - p_i^v}{1 - \hat{p}_i^v} \right)^2 \right] \\ & \approx \sum_v \frac{1}{n} \left(1 + \frac{1 - p_v}{np_v} \right) \quad (\text{from approximation (29)}) \\ & = \frac{1}{n} |V(Pa_{X_i}^G)| + \frac{1}{n^2} \sum_v \frac{1 - p_v}{p_v} \end{aligned} \quad (32)$$

Combining the definition of complexity (2) with equation (32), we have:

$$\sum_{i=1}^m E_{pop}[L_i^2] \approx \frac{C}{n} + \frac{1}{n^2} \sum_{i=1}^m \sum_v \frac{1 - p_v}{p_v} \quad (33)$$

C.2 Approximation of $E_{pop}[L_i L_j]$

There are three possible cases while finding the value of $E[L_i L_j]$. The random variables X_i and X_j might not have any common parents, might have some common parents or one is the parent of other. We start with the case in which X_i and X_j have no common parents. Let $p(v_i, v_j)$ represent the joint probability of $Pa_{X_i}^G = v_i$ and $Pa_{X_j}^G = v_j$.

$$\begin{aligned} E_{pop}[L_i L_j] & = E_{pop} \left[\left(\sum_v 1_{\{Pa_{X_i}^G = v_i\}} L_i^v \right) \left(\sum_{v_j} 1_{\{Pa_{X_j}^G = v_j\}} L_j^{v_j} \right) \right] \\ & = E_{pop} \left[\sum_{v_i, v_j} 1_{\{Pa_{X_i}^G = v_i\}} 1_{\{Pa_{X_j}^G = v_j\}} L_i^v L_j^{v_j} \right] \\ & = \sum_{v_i, v_j} E_{pop} \left[1_{\{Pa_{X_i}^G = v_i\}} 1_{\{Pa_{X_j}^G = v_j\}} L_i^v L_j^{v_j} \right] \\ & = \sum_{v_i, v_j} p(v_i, v_j) E_{pop} \left[L_i^v L_j^{v_j} \right] \\ & \approx \sum_{v_i, v_j} p(v_i, v_j) \times \frac{1}{2np_{v_i}} \times \frac{1}{2np_{v_j}} \quad (\text{from (23)}) \\ & = \sum_{v_i, v_j} \frac{1}{4n^2} \times \frac{p(v_i, v_j)}{p_{v_i} p_{v_j}} \end{aligned} \quad (34)$$

In the case where X_i and X_j have common parents S_{ij} , let S_i represent the parents exclusive to X_i and S_j represent parents exclusive to X_j . Let $p(v_i, v_j, v_{ij})$ represent the joint probability of $Pa_{X_i}^G = v_i$ and $Pa_{X_j}^G = v_j$ and common parent of X_i and X_j ,

$$Pa_{X_{i,j}}^G = v_{ij}.$$

$$\begin{aligned} E_{pop}[L_i L_j] &= E_{pop} \left[\left(\sum_{v_i, v_{ij}} 1_{\{Pa_{X_i}^G = v_i\}} 1_{\{Pa_{X_{ij}}^G = v_{ij}\}} L_i^v \right) \right. \\ &\quad \left. \left(\sum_{v_j, v_{ij}} 1_{\{Pa_{X_j}^G = v_j\}} 1_{\{Pa_{X_{ij}}^G = v_{ij}\}} L_j^v \right) \right] \\ &= E_{pop} \left[\sum_{v_i, v_j, v_{ij}} 1_{\{Pa_{X_i}^G = v_i\}} 1_{\{Pa_{X_j}^G = v_j\}} \right. \\ &\quad \left. 1_{\{Pa_{X_{ij}}^G = v_{ij}\}} L_i^v L_j^v \right] \\ &= \sum_{v_i, v_j, v_{ij}} p(v_i, v_j, v_{ij}) E_{pop} \left[L_i^v L_j^v \right] \\ &\approx \sum_{v_i, v_j, v_{ij}} p(v_i, v_j, v_{ij}) \times \frac{1}{2np(v_i, v_{ij})} \\ &\quad \times \frac{1}{2np(v_j, v_{ij})} \quad (\text{from (23)}) \\ &= \sum_{v_i, v_j, v_{ij}} \frac{1}{4n^2} \times \frac{p(v_i, v_j, v_{ij})}{p(v_i, v_{ij})p(v_j, v_{ij})} \quad (35) \end{aligned}$$

In the case where X_j is a parent of X_i ,

$$\begin{aligned} E_{pop}[L_i L_j] &= E_{pop} \left[\left(\sum_{v_i} 1_{\{Pa_{X_i}^G = v_i\}} x_j L_i^v \right) \left(\sum_{v_j} 1_{\{Pa_{X_j}^G = v_j\}} L_j^v \right) \right] \\ &= E_{pop} \left[\sum_{v_i, v_j} 1_{\{Pa_{X_i}^G = v_i\}} 1_{\{Pa_{X_j}^G = v_j\}} x_j L_i^v \left(x_j \log \frac{p_j^v}{\hat{p}_j^v} \right) \right] \\ &= \sum_{v_i, v_j} p(v_i, v_j, x_j) E_{pop} \left[L_i^v \log \frac{p_j^v}{\hat{p}_j^v} \right] \\ &\approx \sum_{v_i, v_j} p(v_i, v_j, x_j) \times \frac{1}{2np(v_i, x_j)} \\ &\quad \times \frac{1 - p_j^v}{2np_j^v} (\text{from (23)}) \\ &= \sum_{v_i, v_j} \frac{1 - p_j^v}{4n^2} \times \frac{p(v_i, v_j, x_j)}{p(v_i, x_j)p_j^v} \quad (36) \end{aligned}$$

D GENERIC CATEGORICAL VARIABLE

In this section, we generalize our results to any categorical variables (not just binary). The extension from binary to categorical is straightforward. We will have a similar expression for the likelihood ratio statistic:

$$\begin{aligned} L(x) &= \log \left(\frac{\Pr(x; \langle G, \theta \rangle)}{\Pr(x; \langle G, \hat{\theta} \rangle)} \right) \\ &= \sum_{i=1}^m L_i, \end{aligned}$$

where L_i is the contribution of X_i to LR:

$$L_i = \sum_v 1_{\{Pa_{X_i}^G = v\}} L_i^v$$

Instead of writing L_i^v as

$$L_i^v = x_i \log \frac{p_i^v}{\hat{p}_i^v} + (1 - x_i) \log \frac{1 - p_i^v}{1 - \hat{p}_i^v}$$

we write

$$L_i^v = \sum_{o \in V(X_i)} 1_{\{x_i = o\}} \log \frac{p_{io}^v}{\hat{p}_{io}^v},$$

$$p_{io}^v = \Pr(x_i = o | Pa_{X_i}^G = v)$$

Now,

$$\begin{aligned} E_{pop}[L_i^v] &= \sum_{o \in V(X_i)} E \left[p_{io}^v \log \frac{p_{io}^v}{\hat{p}_{io}^v} \right] \\ &= \sum_{o \in V(X_i)} \frac{1 - p_{io}^v}{2n_i^v} \quad (\text{from (24)}) \\ &= \frac{|V(X_i)| - 1}{2n_i^v} \quad (37) \end{aligned}$$

$$\begin{aligned} E_{pop}[L_i] &= \sum_v E[1_{\{Pa_{X_i}^G = v\}} L_i^v | Pa_{X_i}^G = v] \\ &= \sum_v E_{\hat{p}_i^v} \left[E_x \left[1_{\{Pa_{X_i}^G = v\}} L_i^v | \hat{p}_i^v \right] \right] \\ &= \sum_v p_v \frac{|V(X_i)| - 1}{2n_i^v} \quad (\text{from (37)}) \\ &= \sum_v \frac{|V(X_i)| - 1}{2n} + O(n^{-2}) \quad (\text{from (28)}) \\ &= |V(Pa_{X_i})| \times \frac{|V(X_i)| - 1}{2n} + O(n^{-2}) \end{aligned}$$

$$\begin{aligned} E_{pop}[LR] &= \sum_{i=1}^m E_{pop}[L_i] \\ &\approx \sum_{i=1}^m |V(Pa_{X_i})| \times \frac{|V(X_i)| - 1}{2n} + O(n^{-2}) \\ &= \frac{C}{2n} + O(Cn^{-2}) \end{aligned}$$

Hence,

$$E_{pop}[LR] = \frac{C}{2n} + O(Cn^{-2}) \quad (38)$$

Similarly for deriving variance we have,

$$\begin{aligned} E_{pop}[(L_i^v)^2] &= \sum_{o \in V(X_i)} E \left[p_{io}^v \left(\log \frac{p_{io}^v}{\hat{p}_{io}^v} \right)^2 \right] \\ &= \sum_{o \in V(X_i)} \frac{1 - p_{io}^v}{n_i^v} \quad (\text{from (30)}) \\ &= \frac{|V(X_i)| - 1}{n_i^v} \quad (39) \end{aligned}$$

$$\begin{aligned}
E_{pop}[L_i^2] &= \sum_v E[1_{\{Pa_{X_i}^G=v\}}(L_i^v)^2 | Pa_{X_i}^G=v] \\
&= \sum_v E_{\hat{p}_i^v} \left[E_x \left[1_{\{Pa_{X_i}^G=v\}}(L_i^v)^2 | \hat{p}_i^v \right] \right] \\
&= \sum_v p_v \frac{|V(X_i)|-1}{n_i^v} \quad (\text{from (39)}) \\
&= \sum_v \frac{|V(X_i)|-1}{n} + O(n^{-2}) \quad (\text{from (28)}) \\
&= |V(Pa_{X_i})| \times \frac{|V(X_i)|-1}{n} + O(n^{-2})
\end{aligned}$$

Hence,

$$\begin{aligned}
\sum_{i=1}^m E_{pop}[L_i^2] &= \sum_{i=1}^m |V(Pa_{X_i})| \times \frac{|V(X_i)|-1}{n} + O(n^{-2}) \\
&= \frac{C}{n} + O(Cn^{-2})
\end{aligned}$$

$$\begin{aligned}
\text{Var}_{pop}(L) &= E_{pop}[L^2] - (E_{pop}[L])^2 \\
E_{pop}[L^2] &= \sum_{i=1}^m E[L_i^2] + 2 \sum_{1 \leq i < j \leq m} E[L_i L_j]
\end{aligned}$$

Similar to the derivations of $\sum E_{pop}[L_i]$ and $\sum E_{pop}[L_i^2]$, we will have

$$\sum_{i,j} E_{pop}[L_i L_j] = \frac{C^2}{4n^2} + O(C^2 n^{-2})$$

Hence, for categorical variables:

$$\text{Var}_{pop}[LR] = \frac{C}{n} + O(C^2 n^{-2}) \quad (40)$$

E NAIVE BAYES

In section 5.2, while deriving the variance, we haven't calculated the exact value of the $O(C^2 n^{-2})$ term. From the released model, it is possible to calculate the exact value of this term. Here we derive the exact value of the $O(C^2 n^{-2})$ term, when the released model is a Naive Bayes model. Let the number of attributes in the model be equal to m . Hence, the complexity of the model is $C = 2m - 1$. Let X_1 be the class variable and $p_i^1 = Pr(X_i = 1 | X_1 = 1)$. Then, using

equation (23) we have:

$$\begin{aligned}
E_{pop}(L) &= E_{pop} \left[x_1 \log \frac{p_1}{\hat{p}_1} + (1-x_1) \log \frac{1-p_1}{1-\hat{p}_1} \right. \\
&\quad \left. + x_1 \sum_{i=2}^m \left(x_i \log \frac{p_i^1}{\hat{p}_i^1} + (1-x_i) \log \frac{1-p_i^1}{1-\hat{p}_i^1} \right) \right. \\
&\quad \left. + (1-x_1) \sum_{i=2}^m \left(x_i \log \frac{p_i^0}{\hat{p}_i^0} + (1-x_i) \log \frac{1-p_i^0}{1-\hat{p}_i^0} \right) \right] \\
&= \frac{1}{2n} + \sum_{i=2}^m \left[p_1 \times \frac{1}{2np_1} + \frac{1}{2n^2} \left[\frac{1-p_1}{p_1} \right] \right] \\
&\quad + \sum_{i=2}^m \left[(1-p_1) \times \frac{1}{2n(1-p_1)} + \frac{1}{2n^2} \left[\frac{p_1}{1-p_1} \right] \right] \\
&= \frac{2m-1}{2n} + O(mn^{-2}) \\
&= \frac{C}{2n} + O(Cn^{-2}) \quad (41)
\end{aligned}$$

We can calculate the exact value of $E_{pop}(L^2)$ using the equations (29), (35) and (36) as below :

$$\begin{aligned}
E_{pop}(L^2) &= E_{pop} \left[\left[x_1 \log \frac{p_1}{\hat{p}_1} + (1-x_1) \log \frac{1-p_1}{1-\hat{p}_1} \right. \right. \\
&\quad \left. \left. + x_1 \sum_{i=2}^m \left(x_i \log \frac{p_i^1}{\hat{p}_i^1} + (1-x_i) \log \frac{1-p_i^1}{1-\hat{p}_i^1} \right) \right. \right. \\
&\quad \left. \left. + (1-x_1) \sum_{i=2}^m \left(x_i \log \frac{p_i^0}{\hat{p}_i^0} \right. \right. \right. \\
&\quad \left. \left. \left. + (1-x_i) \log \frac{1-p_i^0}{1-\hat{p}_i^0} \right) \right]^2 \right] \\
&= \frac{1}{n} + \sum_{i=2}^m \left[p_1 \times \frac{1}{np_1} + \frac{1}{n^2} \left[\frac{1-p_1}{p_1} \right] \right] \\
&\quad + \sum_{i=2}^m \left[(1-p_1) \times \frac{1}{n(1-p_1)} + \frac{1}{n^2} \left[\frac{p_1}{1-p_1} \right] \right] \\
&\quad + 2 \left[\binom{m-1}{2} \times \frac{p_1}{4n^2 \hat{p}_1^2} \right. \\
&\quad \left. + \binom{m-1}{2} \times \frac{1-p_1}{4n^2 (1-\hat{p}_1)^2} \right. \\
&\quad \left. + \frac{(m-1)(1-p_1)}{4n^2} + \frac{(m-1)p_1}{4n^2} \right] \\
&= \frac{2m-1}{n} + \frac{(m-1)(m-2)}{4n^2} \left[\frac{p_1}{\hat{p}_1^2} \right. \\
&\quad \left. + \frac{1-p_1}{(1-\hat{p}_1)^2} \right] + O(mn^{-2}) \\
&\approx \frac{C}{n} + \frac{m^2}{4n^2} \left[\frac{1}{p_1(1-p_1)} \right] + O(mn^{-2}) \quad (42)
\end{aligned}$$

Combining equations (41) and (42), we have the variance for Naive Bayes as:

$$\begin{aligned}
\text{Var}_{pop}(L) &= E_{pop}(L^2) - (E_{pop}(L))^2 \\
&= \frac{C}{n} + \frac{m^2}{4n^2} \left[\frac{1}{p_1(1-p_1)} - 4 \right] + O(mn^{-2}) \\
&\approx \frac{C}{n} + O(C^2n^{-2})
\end{aligned} \tag{43}$$

F FISHER INFORMATION - PARAMETER ESTIMATION

Fisher information quantifies the amount of information a random variable carries about the parameter(s) θ of the probability distribution from which it is generated.

$$I(\theta) = -E_{\theta}(\nabla^2 l(\theta)),$$

where $I(\theta)$ is Fisher information, and $l(\theta)$ is the log-likelihood function for θ .

If $\hat{\theta}$ is a Maximum Likelihood Estimate of θ , then it is known that

$$\hat{\theta} = \text{Normal}(\theta, I(\hat{\theta})^{-1}).$$

The log-likelihood functions of parameter θ from a PGM $\langle G, \theta \rangle$, given a sample x are typically of the form:

$$\begin{aligned}
l(\theta) &= \log [\text{Pr}(x; \langle G, \theta \rangle)] \\
&= \sum_{i=1}^m l_i
\end{aligned}$$

where l_i is contribution of X_i to the likelihood function:

$$\begin{aligned}
l_i &= \sum_{v \in V(Pa_{X_i}^G)} 1_{\{Pa_{X_i}^G = v\}} l_i^v \\
l_i^v &= \sum_{o \in V(X_i)} 1_{\{x_i = o\}} \log p_{io}^v \\
l &= \sum_{i,v,o} f_{i,v,o}(x_1, x_2, \dots, x_m) \log(p_{io}^v),
\end{aligned}$$

where $f_{i,v,o}$ are activator functions (some combination of x_i 's) for the parameter p_{io}^v .

$$I(p) = -E_p(\nabla^2 l(p))$$

All the non-diagonal elements of the information matrix are zero, because:

$$\frac{\partial}{\partial p_{io}^v} \frac{\partial}{\partial p_{jo}^v} \left[\sum_{i,v,o} f_{i,v,o}(x_1, x_2, \dots, x_m) \log(p_{io}^v) \right] = 0, \forall i \neq j$$

This implies that all the standard normal variables used to represent frequencies in pool are pair-wise independent i.e. all estimation errors are independent. The power for inference is provided by finite sample estimation error. These two facts together explain why the complexity of a PGM equals to the number of independent parameters required to define probability distribution of the graph.